Supplementary Information

Correlating chemical sensitivity and basal gene expression reveals mechanism of action

Matthew G. Rees[1], Brinton Seashore-Ludlow[1,3], Jaime H. Cheah[1,4], Drew J. Adams[1,5], Edmund V. Price[1,6], Shubhroz Gill[1], Sarah Javaid[2], Matthew E. Coletti[1], Victor L. Jones[1], Nicole E. Bodycombe[1,7], Christian K. Soule[1,4], Benjamin Alexander[1], Ava Li[1], Philip Montgomery[1], Joanne D. Kotz[1], C. Suk-Yee Hon[1], Benito Munoz[1], Ted Liefeld[1,8], Vlado Dančík[1], Daniel A. Haber[2], Clary B. Clish[1], Joshua A. Bittker[1], Michelle Palmer[1,9], Bridget K. Wagner[1], Paul A. Clemons[1,*], Alykhan F. Shamji[1,*], and Stuart L. Schreiber[1,*]

[1]Broad Institute, Cambridge, MA, 02142, USA

[2]Massachusetts General Hospital Cancer Center, 149 13th St, Charlestown, MA, 02129, USA

[3]Present address: Chemical Biology Consortium Sweden, Science for Life Laboratory Stockholm, Division of Translational Medicine and Chemical Biology, Department of Medical Biochemistry and Biophysics, Karolinska Institutet, Solna, Sweden

[4]Present address: Koch Institute for Cancer Research at MIT, Cambridge, MA, 02139, USA

[5]Present address: Department of Genetics and Genome Sciences, Case Western Reserve University School of Medicine, Cleveland, OH, 44106, USA

[6]Present address: Novartis Institutes for Biomedical Research, Emeryville, CA, 94608, USA

[7]Present address: Pfizer, Cambridge, MA, 02139, USA

[8]Present address: UC San Diego School of Medicine, La Jolla, CA, 92093, USA

[9]Present address: ImmunoGen, Waltham, MA, 02451, USA

*Correspondence: pclemons@broadinstitute.org (P.A.C.), ashamji@broadinstitute.org (A.F.S.), stuart_schreiber@harvard.edu (S.L.S.)

Supplementary Results

Supplementary Tables

Supplementary Table 1. Selected examples of single transcripts most correlated with response to small molecules yielding interpretable biology.

	small molecule	reported targets	most correlated transcript	number of significant outliers
direct targets; high expression correlates with sensitivity	ABT-199	*BCL2*	*BCL2*	3
	nintedanib	*FGFR1;FGFR2;FGFR3;FLT1;FLT3;KDR;PDGFRA;PDGFRB*	*PDGFRA*	9
	Ki8751	*KDR;KIT;PDGFRA*	*PDGFRA*	9
	imatinib	*ABL1;BCR;KIT;PDGFRA*	*PDGFRA*	9
	sunitinib	*FLT1;FLT3;KDR;KIT;PDGFRA;PDGFRB*	*PDGFRA*	9
	ML239	novel	*FADS2*	1
	DNMDP	novel	*PDE3A*	2
direct targets; low expression correlates with sensitivity	GMX-1778; CAY10618	*NAMPT*	*NAMPT*	8
	erastin	*SLC7A11;VDAC1;VDAC2*	*SLC7A11*	20
proximal to direct target; high expression correlates with sensitivity	tandutinib	*FLT3;KIT*	*PDGFRA*	9
	quizartinib	*FLT3*	*PDGFRA*	9
	tivozanib	*FLT1;FLT3;KDR*	*PDGFRA*	9
	neratinib	*EGFR;ERBB2*	*GRB7*	11
	birinapant	*DIABLO;XIAP*	*RIPK1*	1
proximal to direct target; low expression correlates with sensitivity	GDC-0941	*PIK3CA;PIK3CB;PIK3CD;PIK3CG*	*IRS2*	0
	MLN2480	*ARAF;BRAF;RAF1*	*RRAS2*	10
	simvastatin; lovastatin	*HMGCR*	*HMGCS1*	2
	tanespimycin	*HSP90AA1*	*NQO1*	1
	zebularine	*DNMT1*	*UCK2*	17
	YM-155	*BIRC5*	*SLC35F2*	1
	RITA	*MDM2;TP53*	*SULT1A1*	1
	austocystin D	novel	*CYP2J2*	4
metabolic inactivation / drug efflux	PI-103	*MTOR;PIK3CA;PIK3CB;PIK3CD;PIK3CG;PRKDC*	*ABCC3*	30
	SNS-032	*CDK16;CDK17;CDK2;CDK7;CDK9;CDKL5*	*ABCB1*	3
	NSC23766	*RAC1;TIAM1;TRIO*	*ABCB1*	3
	obatoclax	*BCL2;BCL2L1;MCL1*	*BLVRB*	26
	YM-155	*BIRC5*	*ABCB1*	3
	BRD1378; BRD5468	novel	*ABCC1*	10
selected other connections	PF-184	*IKBKB*	*SLFN11*	7
	topotecan; SN-38	*TOP1*	*SLFN11*	7
	gemcitabine	*CMPK1;RRM1;TYMS*	*SLFN11*	7
	clofarabine	*POLA1;POLA2;POLE;RRM1*	*SLFN11*	7
	PD318088	*MAP2K1;MAP2K2*	*ETV4*	5
	dabrafenib; GDC-0879; PLX-4720; vemurafenib	*BRAF*	*TRIM51*	8
	BRD1378; BRD5468	novel	*MGLL*	2

Number of selected outliers: number of small molecules (of 481) for which the transcript is both a Tukey outlier and significantly correlated after Bonferroni correction ($|z| > 5.83$). Selected other connections, see supplementary references [1,5,9,10].

Supplementary Data Set 1. The cancer cell-line panel.

Description of the cancer cell lines (CCLs) profiled in this experiment, including annotations from the CCLE[1] for lineage and histology and experimental growth conditions (including media composition).

Supplementary Data Set 2. The small-molecule informer set.

Description of the small-molecule informer set profiled in this experiment, including concentrations used, protein target or activity, source and vendor information, and structure.

Supplementary Data Set 3. Area-under curve values for 481 small molecules across 823 unique CCLs.

Supplementary Data Set 4. All transcripts significantly correlated with small-molecule sensitivity across all CCLs, non-HL CCLs, and HL CCLs.

A Bonferroni-corrected significance cutoff of $|z| > 5.83$, representing a two-tailed distribution with family-wise error-rate $\alpha < 0.025$ in each tail, was used.

Supplementary Data Set 5. Significant lineage-specific correlation values.

All significant values where the absolute value of the z-scored Pearson correlation was greater than the value across all CCLs and non-HL CCLs are included.

Supplementary Data Set 6. Correlations for 660 annotated compound-target pairs across all CCLs, non-HL CCLs, and HL CCLs.

For compound-target pairs, the transcript rank (of 18,543 transcripts), z-scored Pearson correlation, and significance ($|z| > 3.96$; Bonferroni-corrected, two-tailed distribution with family-wise error-rate $\alpha < 0.025$ in each tail) are included.

Supplementary Data Set 7. Expression-sensitivity correlations for *TNFRSF12A* with 481 small molecules across all CCLs.

Included are the number of CCLs tested per small molecule; *TNFRSFS12A* transcript rank (see **Supplementary Fig. 1b**); the Pearson expression-sensitivity correlation; the z-scored Pearson correlation; minimum, median, mean, maximum, and standard deviation of z-scored correlations from permutation testing (65,536 permutations); results of Kolmogorov-Smirnov test for normality of permutation results; empirical p-value from permutation testing; and estimated p-value from the normal cumulative distribution function.

Supplementary Data Set 8. Transcript loadings from principal component analyses (PCA).

Results are from PC_A1 (first PC from PCA of the entire 18,543 transcript × 481 small molecule correlation matrix across all CCLs), PC_B1 (first PC from PCA of the correlation matrix excluding HL CCLs), and PC_B2 (second PC from PCA of the correlation matrix excluding HL CCLs). The number of small molecules to which each gene was significantly correlated (excluding HL CCLs) was calculated using a Bonferroni-corrected, two-tailed distribution with family-wise error-rate $\alpha < 0.025$ in each tail ($|z| > 5.83$).

Supplementary Data Set 9. Small-molecule scores from principal component analyses.

Supplementary Data Set 10. GSEA results with PC_B2 gene loadings as the input using the C2 and C5 gene sets.

See www.broadinstitute.org/gsea/doc/GSEAUserGuideTEXT.htm#_Viewing_Analysis_results for analysis description.

Supplementary Data Set 11. Correlations across all 481 small molecules for 654 individual transcripts most correlated with response to at least one small molecule.

Included are the number of CCLs tested per small molecule; transcript rank; the Pearson expression-sensitivity correlation; the z-scored Pearson correlation; minimum, median, mean, maximum, and standard deviation of z-scored correlations from permutation testing (≥16,384 permutations); results of Kolmogorov-Smirnov test for normality of permutation results; empirical p-value from permutation testing; and estimated p-value from the normal cumulative distribution function.

Supplementary Data Set 12. GSEA results with austocystin D expression-sensitivity correlations (excluding HL CCLs) as the input using the C2 and C5 gene sets.

See www.broadinstitute.org/gsea/doc/GSEAUserGuideTEXT.htm#_Viewing_Analysis_results for analysis description.

Supplementary Data Set 13. Raw results from profiling cellular lipids in NCIH661 cells.

Results are from 24-hour treatment with 2 μM ML239, 2 μM SC-26196, co-treatment, or DMSO, with individual replicates numbered across columns. Metabolite IDs match those from The Human Metabolome Database (www.hmdb.ca).

Supplementary Data Set 14. Mapping of accession numbers for the file CCLE_Expression_Entrez_2012-10-18.res to the gene symbols used in this analysis.

Supplementary Figures

Supplementary Figure 1a

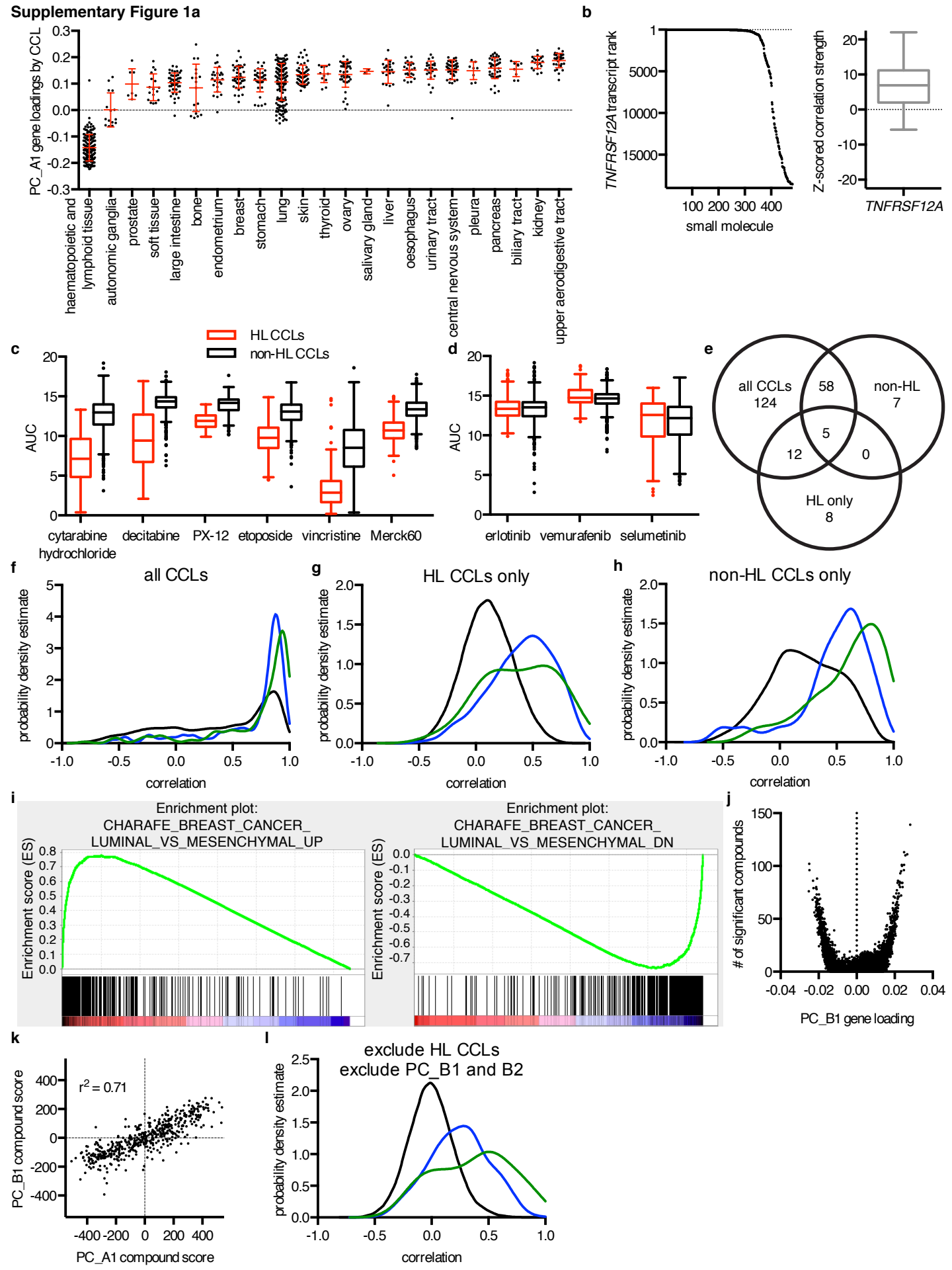

Supplementary Figure 1. Groups of CCLs whose global sensitivity or expression profiles dominate pattern of correlation.

(**a**) Pearson correlation of 18,543 PC_A1 gene loadings with basal expression levels of these 18,543 transcripts across 823 CCLs separated by lineage annotation from the Cancer Cell Line Encyclopedia[1]. (**b**) Z-scored Pearson correlation transcript rank (out of 18,543) and value for *TNFRSF12A* across 481 small molecules. (**c**) Exemplar small molecules that are selective for HL CCLs, and therefore strongly associated with features of these CCLs (e.g., *TNFRSF12A* expression and PC_A1 score). (**d**) Exemplar small molecules that are toxic to a proportion of CCLs (minimum AUC < 8) but are not selective for HL CCLs. (**e**) Venn diagram of significant ($|z| > 3.96$, representing two-tailed Bonferroni-corrected significance) Z-scored Pearson correlation coefficients between 660 annotated small-molecule-target pairs across all CCLs, non-HL CCLs, and HL CCLs. (**f–h**) Comparison of similarities in genome-wide patterns of 18,543 sensitivity-expression correlations for small molecules sharing no targets (black), some targets (blue), or all targets (green) in (**f**) all CCLs, (**g**) HL CCLs only, or (**h**) non-HL CCLs only. (**i**) Top 'up' and 'down' pathway result from Gene Set Enrichment Analysis (GSEA) of PC_B2 gene loadings. See **Supplementary Data Set 10**. (**j**) 18,543 gene loadings for PC_B1 (excluding HL CCLs), and the number of compounds to which each gene has a significant expression-sensitivity correlation (Bonferroni-corrected, two-tailed distribution with family-wise error-rate $\alpha < 0.025$ in each tail). (**k**) Compound scores for PC_A1 (all CCLs) and PC_B1 (excluding HL CCLs) across 481 small molecules. (**l**) Comparison of similarities in genome-wide patterns of 18,543 sensitivity-expression correlations for small molecules sharing no targets (black), some targets (blue), or all targets (green) in non-HL CCLs with exclusion of PC_A1 and PC_B2.

Supplementary Figure 2a

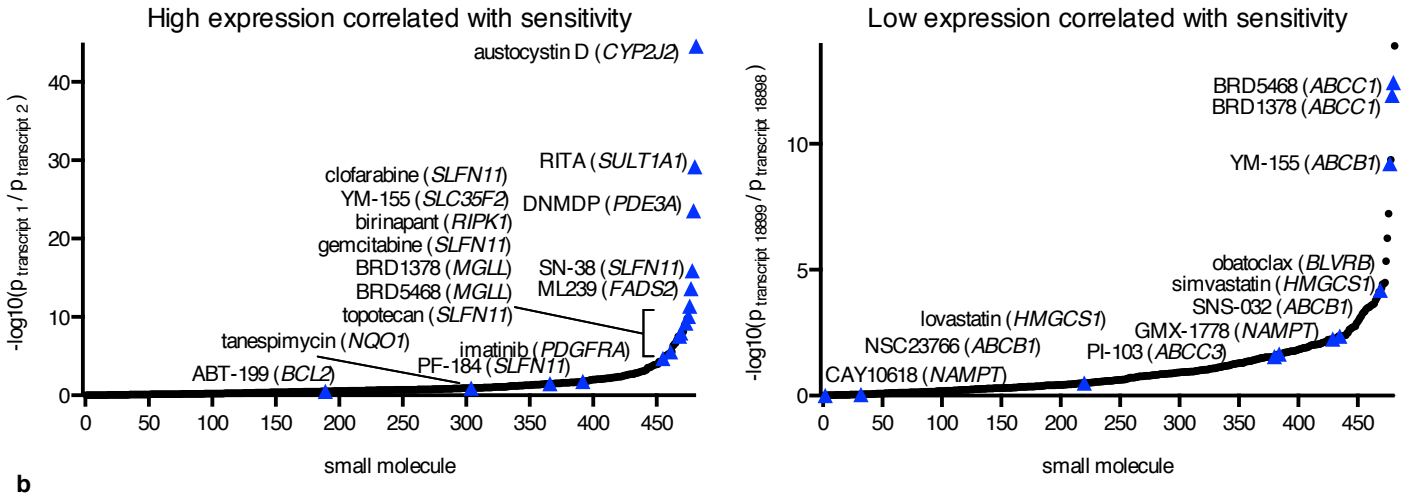

b

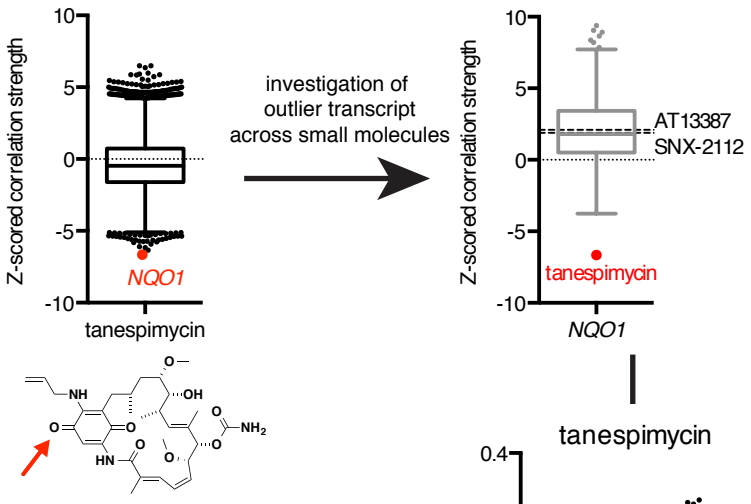

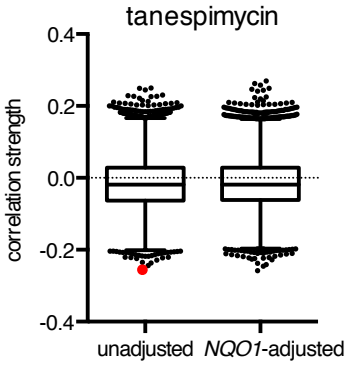

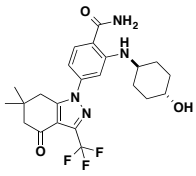

non-quinone

	small molecule	r	z(r)	rank
1	tanespimycin	-0.255	-6.65	1
2	GDC-0879	-0.148	-3.77	1002
…				
247	SNX-2112	0.073	1.88	16589
…				
268	AT13387	0.117	2.09	17220
…				
481	BRD-K34222889	0.353	9.38	18532

biological validation of novel MoA,
investigation of additional correlated transcripts,
multigene analyses, etc.

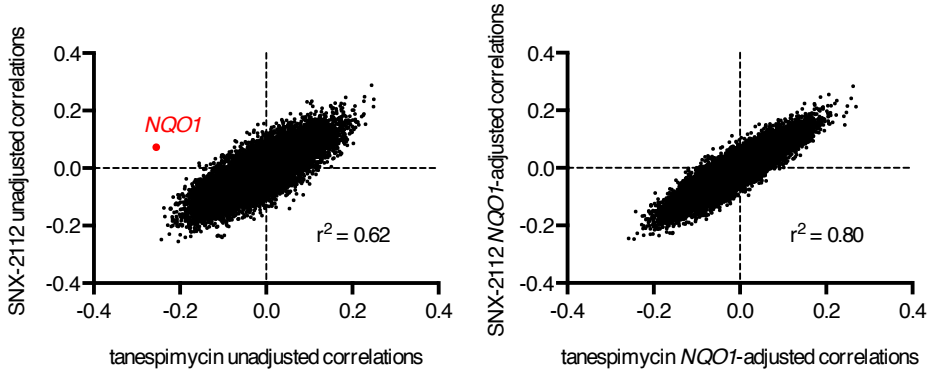

Supplementary Figure 2c

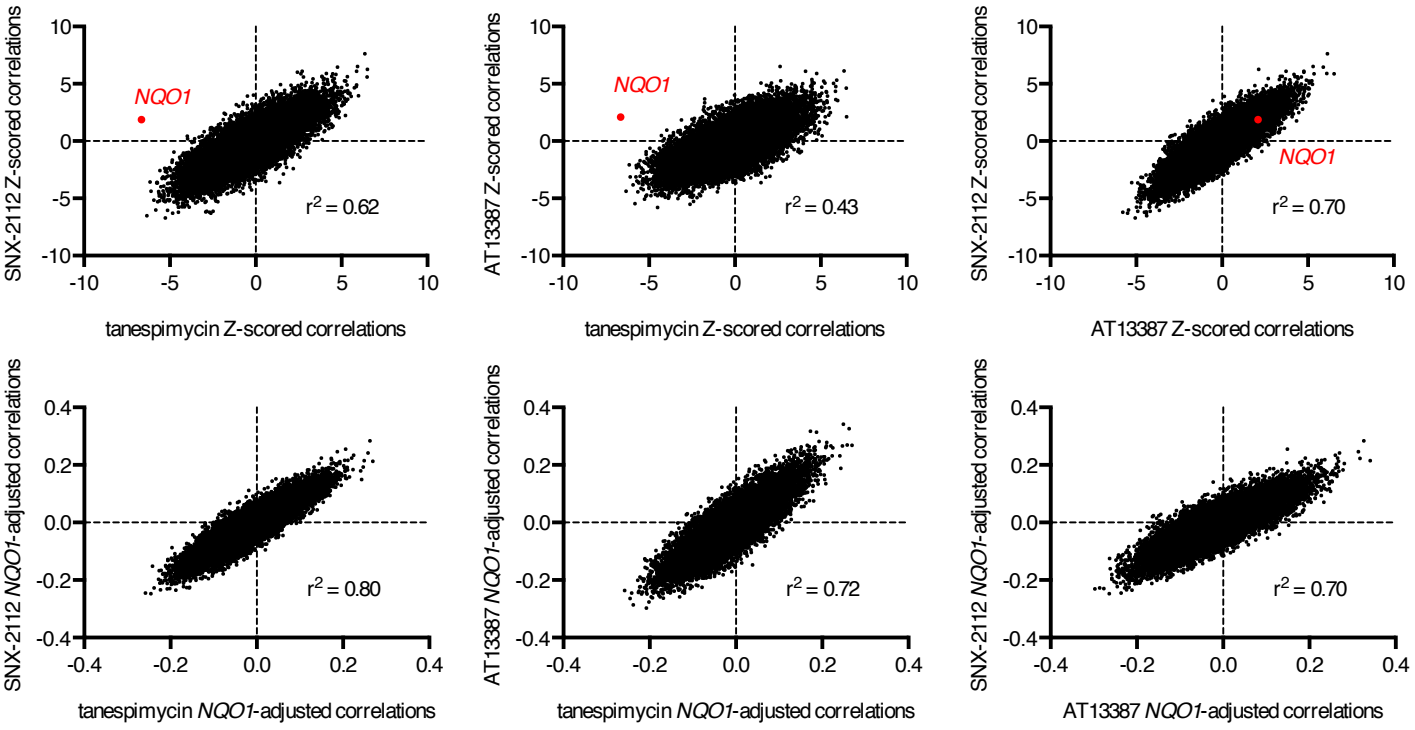

	Gene	tanespimycin *NQO1*-adj.	SNX-2112 *NQO1*-adj.
1	*ADAT2*	-0.258	-0.245
2	*NAA16*	-0.245	-0.247
3	*METTL21D*	-0.242	-0.152
4	*NSMCE4A*	-0.238	-0.227
5	*USP7*	-0.228	-0.197
6	*L2HGDH*	-0.226	-0.167
7	*TAF5*	-0.225	-0.211
8	*CNTRL*	-0.223	-0.233
9	*ZBED4*	-0.223	-0.202
10	*PASK*	-0.222	-0.167
	…		
18889	*VLDLR*	0.220	0.224
18890	*LEPROT*	0.223	0.184
18891	*CREBRF*	0.225	0.234
18892	*YIPF5*	0.241	0.180
18893	*GABARAPL1*	0.243	0.149
18894	*MITF*	0.247	0.192
18895	*SQSTM1*	0.249	0.215
18896	*GNS*	0.258	0.242
18897	*ATP10A*	0.263	0.284
18898	*ATP6V0E1*	0.269	0.213

Supplementary Figure 2d

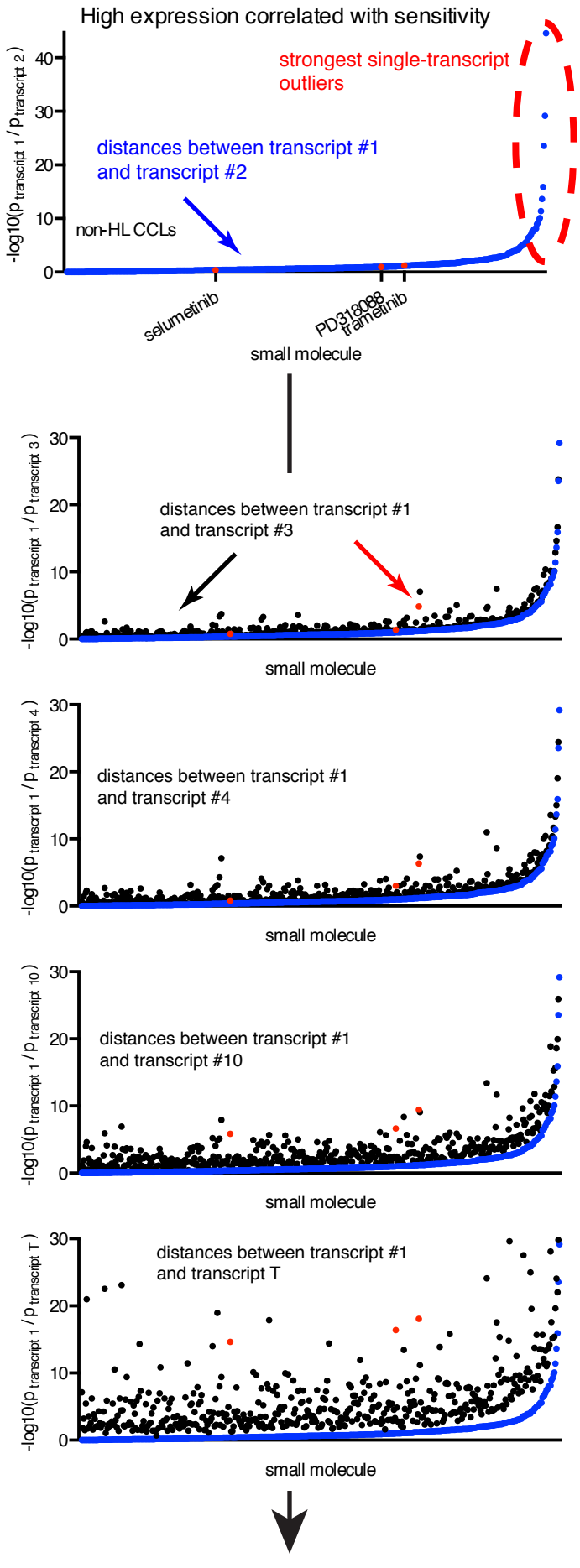

small molecule	$-\log_{10}\left(\frac{p_{transcript\ 2}}{p_{transcript\ T}}\right)$
austocystin D	38.20
dabrafenib	32.57
GDC-0879	27.61
PLX-4720	26.92
afatinib	24.00
dasatinib	23.01
lapatinib	22.48
N9-isopropylolomoucine	22.04
neratinib	21.01
canertinib	20.99
nutlin-3	19.98
RITA	18.74
erlotinib	18.62
ABT-199	17.36
trametinib	16.85
PD318088	15.40
gefitinib	15.29
BI-2536	15.25
ABT-737	14.30
selumetinib	14.27

Supplementary Figure 2d (continued)

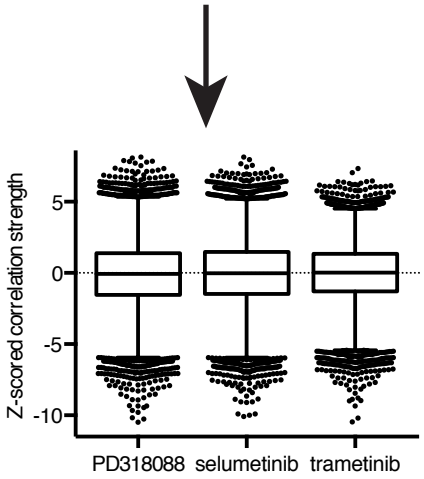

Transcript	z(r)	rank	z(r)	rank	z(r)	rank
SH3TC2	-10.3	2	-9.90	3	-10.5	1
ETV4	-10.5	1	-9.89	4	-10.2	2
ATP10B	-9.80	4	-9.99	2	-8.88	6
SPRY2	-10.2	3	-9.04	7	-9.35	3
CEACAM1	-9.33	7	-10.1	1	-8.79	7
SPRY4	-9.33	8	-9.05	6	-8.95	5
DUSP6	-9.66	5	-8.88	8	-8.44	8
ITGA6	-9.46	6	-9.09	5	-7.87	13
…						

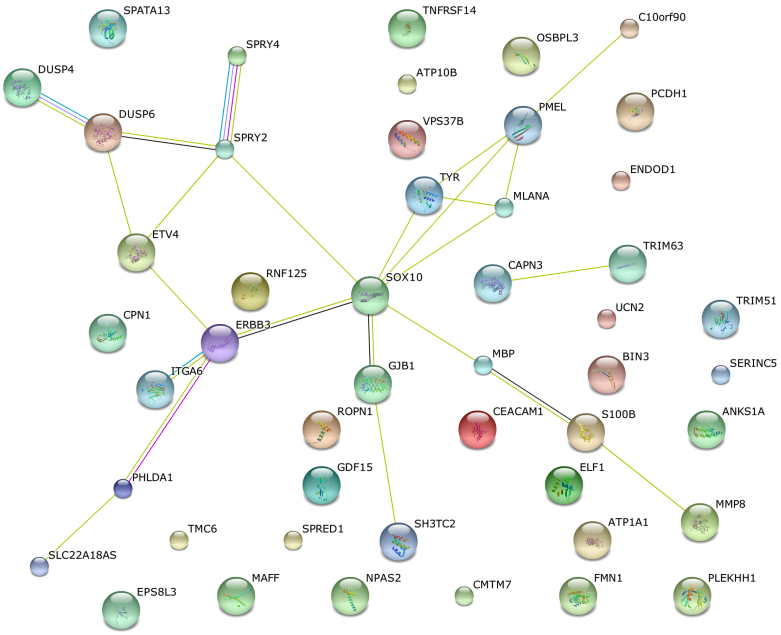

Supplementary Figure 2. MoA analysis, and its application to the HSP90 inhibitor tanespimcyin.

(**a**) Difference between the most- and second-most-associated transcripts correlated with sensitivity to each small molecule in non-HL CCLs calculated from the normal cumulative distribution function for each small molecule. Negative (high expression correlates with sensitivity) and positive (low expression correlates with sensitivity) correlations are treated separately. Small molecules in **Supplementary Table 1** and discussed in text and figures are shown as blue triangles. (**b–c**) Overview of analysis of outlier transcripts. (**b**) Expression–sensitivity correlations for tanespimycin implicate *NQO1*, and *NQO1* expression is uniquely associated to tanespimycin across small molecules. The NQO1 enzyme converts tanespimycin (red arrow) into a hydroquinone that is a more potent HSP90 inhibitor [2,3], while two other HSP90 inhibitors, SNX-2112 and AT13387, do not contain quinone moieties. A comparison of correlation profiles between HSP90 inhibitors with and without adjustment for expression of *NQO1* using semi-partial correlation reveals that *NQO1* is a critical distinguishing factor between the global correlation profiles of HSP90 inhibitors. (**c**) Complete adjusted and unadjusted correlation profile comparisons between HSP90 inhibitors, and list of transcripts most associated with tanespimycin and SNX-2112 after adjustment for *NQO1* expression. Such lists may be used in downstream analyses (e.g., pathway or network analysis, comparing correlation results across small molecules that are not HSP90 inhibitors, etc.). (**d**) Application of MoA analysis to identify small molecules with multi-transcript correlation outliers. The top panel demonstrates the approach used in **b**; the same approach can be used to calculate the distance between the top-ranked transcript and any outlier transcript (*e.g.*, Tukey outliers; transcript T). Small molecules implicated by this approach, but not by a single-transcript approach, can be

prioritized (*e.g.*, a ranked list of compounds by $-\log10(p_{transcript\ 2}/p_{transcript\ T})$) for further investigation. Expression-sensitivity correlations highlighting the top-ranked transcripts associated with response to 3 MEK 1/2 inhibitors are shown, along with a STRING network visualization of interactions between 48 proteins encoded by 50 transcripts most correlated with response, are shown[4]. Connected nodes include multiple proteins that have been previously associated with response to MEK 1/2 inhibitors[5]. Boxplot outlier points represent Tukey outliers.

Supplementary Figure 3a

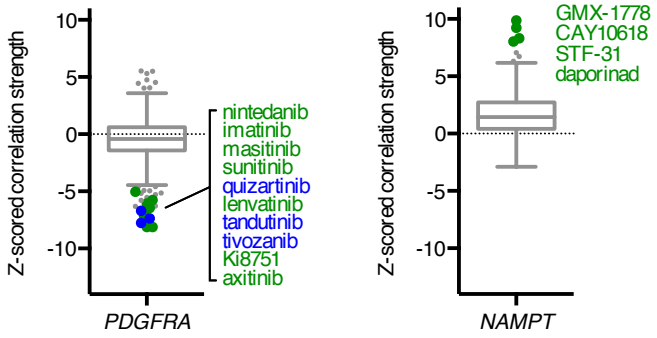

b

transcript	small molecule	r	z(r)	p-value	rank
BCL2	ABT-199	-0.478	-10.3	<8.0E-08	1
	ABT-737	-0.352	-9.00	<8.0E-08	7
	navitoclax	-0.288	-7.53	<8.0E-08	4
	obatoclax	-0.156	-4.03	0.000028	758
	TW-37	-0.122	-3.07	0.0011	2175
	BRD-M00053801	-0.0795	-1.59	0.055	2812
	gossypol	-0.0393	-0.982	0.16	7745

c

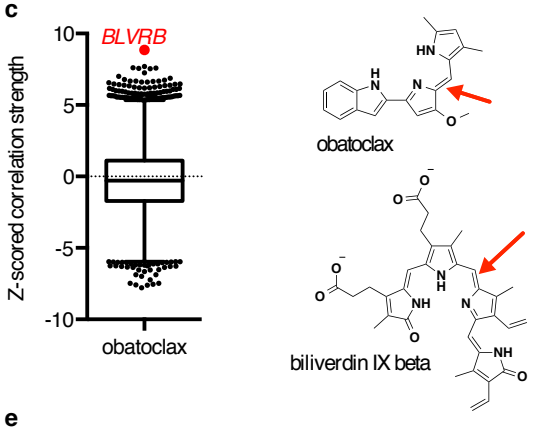

d

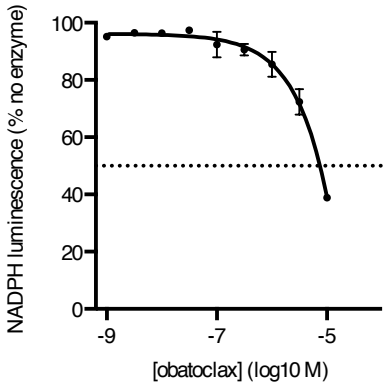

e

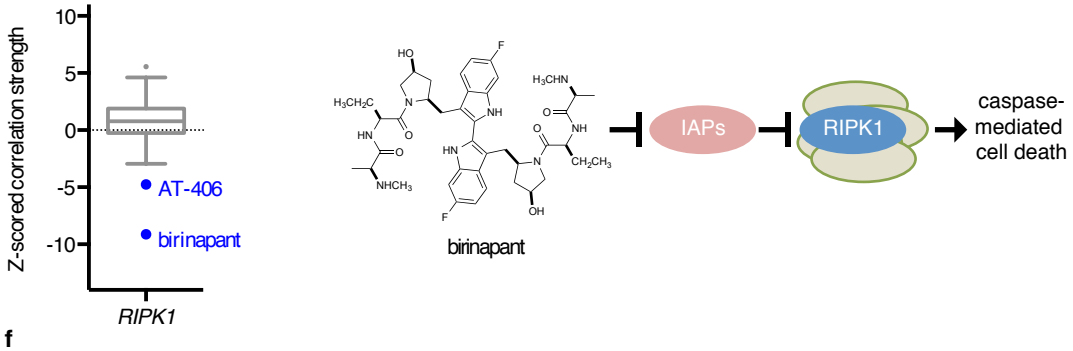

f

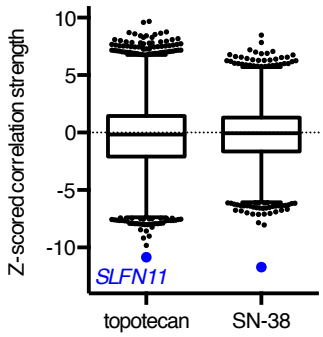

Supplementary Figure 3. MoA analysis illuminates small-molecule targets and target pathways, and informs similarities and differences between groups of compounds.

(**a**) Expression-sensitivity correlations for *PDGFRA* and *NAMPT*. (**b**) Comparison of transcript correlations between *BCL2* and annotated BCL2-family inhibitors. For ABT-199, ABT-737, and navitoclax, an empirical p-value was used because the correlations failed a Kolmogorov-Smirnov test for normality; instead, results from 1.3×10^7 permutations of CCL labels are included. All other p-values are estimated for a two-tailed distribution with Bonferroni correction. (**c**) Expression-sensitivity correlations for obatoclax, the structure of obatoclax, and structure of the canonical BLVRB substrate biliverdin IX beta. (**d**) Activity of 0.4 μg BLVRB at varying concentrations of obatoclax. Each point is mean ± s.d. for n = 3 independent experiments. (**e–f**) Expression-sensitivity correlations for (**e**) *RIPK1* and (**f**) the topoisomerase I inhibitors topotecan and SN-38. Z-scored Pearson correlations are shown. Boxplot outlier points represent Tukey outliers. Reactive functionalities are depicted with a red arrow. Direct target connections are shown in green, target pathway connections in blue, and mechanisms of metabolism in red.

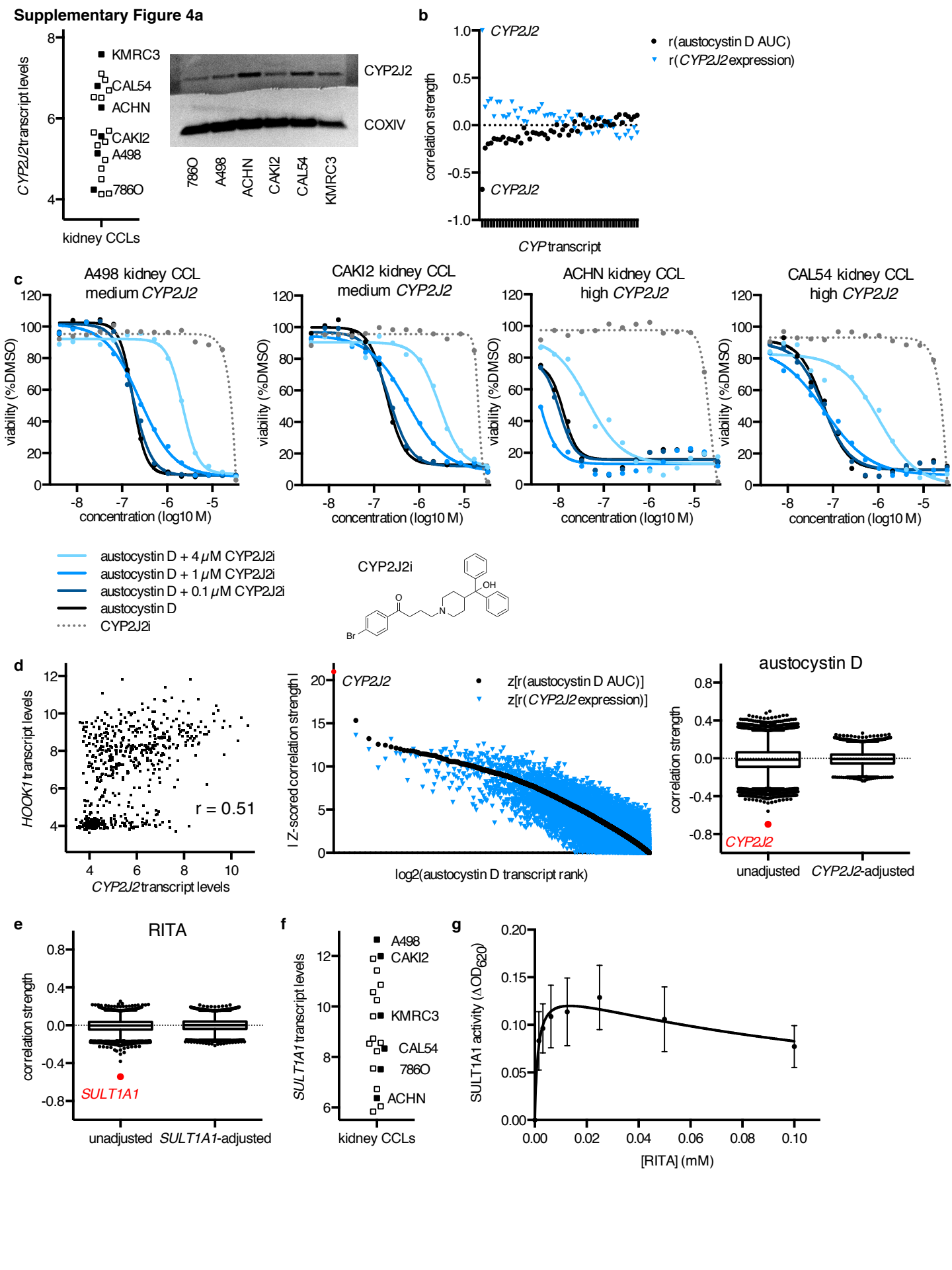
Supplementary Figure 4a
CYP2J2 transcript levels
kidney CCLs
KMRC3
CAL54
ACHN
CAKI2
A498
786O
CYP2J2
COXIV
b
CYP2J2
r(austocystin D AUC)
r(CYP2J2 expression)
correlation strength
CYP transcript
c
A498 kidney CCL
medium CYP2J2
CAKI2 kidney CCL
medium CYP2J2
ACHN kidney CCL
high CYP2J2
CAL54 kidney CCL
high CYP2J2
viability (%DMSO)
concentration (log10 M)
austocystin D + 4 μM CYP2J2i
austocystin D + 1 μM CYP2J2i
austocystin D + 0.1 μM CYP2J2i
austocystin D
CYP2J2i
CYP2J2i
d
HOOK1 transcript levels
CYP2J2 transcript levels
r = 0.51
| Z-scored correlation strength |
z[r(austocystin D AUC)]
z[r(CYP2J2 expression)]
log2(austocystin D transcript rank)
austocystin D
correlation strength
unadjusted
CYP2J2-adjusted
e
RITA
SULT1A1
unadjusted
SULT1A1-adjusted
f
SULT1A1 transcript levels
kidney CCLs
g
SULT1A1 activity (ΔOD620)
[RITA] (mM)

Supplementary Figure 4. MoA analysis reveals novel mechanisms of small-molecule metabolic activation.

(**a**) Transcript and protein levels of *CYP2J2* across renal CCLs, with CCLs in **c** and **Figure 2b** indicated (filled black squares). For uncropped gel image, see **Supplementary Figure 8a**. (**b**) Pearson correlation of 53 CYP transcripts with austocystin D sensitivity (black circles) and with *CYP2J2* transcript levels (blue triangles) across 592 non-HL CCLs assayed for austocystin D sensitivity. (**c**) Cytotoxicity of austocystin D and a selective CYP2J2 inhibitor (CYP2J2i) across renal CCLs and effects of co-treatment with CYP2J2i. Each point shows the mean of 2 independent experiments with 2 technical replicates each. (**d**) Co-expression plot for *CYP2J2* and *HOOK1* in 592 non-HL CCLs assayed for austocystin D sensitivity, absolute value of Z-scored expression–sensitivity Pearson correlations for austocystin D (dots), with correlation of each transcript to *CYP2J2* indicated (blue triangles), and expression-sensitivity correlations for austocystin D with and without adjustment for expression of *CYP2J2* using semi-partial correlation. Pearson correlations are shown. Boxplot outlier points represent Tukey outliers. (**e**) Expression-sensitivity correlations for RITA with and without adjustment for expression of *SULT1A1* using semi-partial correlation. Pearson correlations are shown. Boxplot outlier points represent Tukey outliers. (**f**) Transcript levels of *SULT1A1* across renal CCLs, with CCLs in **Figure 2e** indicated (filled black squares). (**g**) Activity of 1 μg SULT1A1 at varying concentrations of RITA. Each point is mean ± s.d. for n = 3 independent experiments.

Supplementary Figure 5a

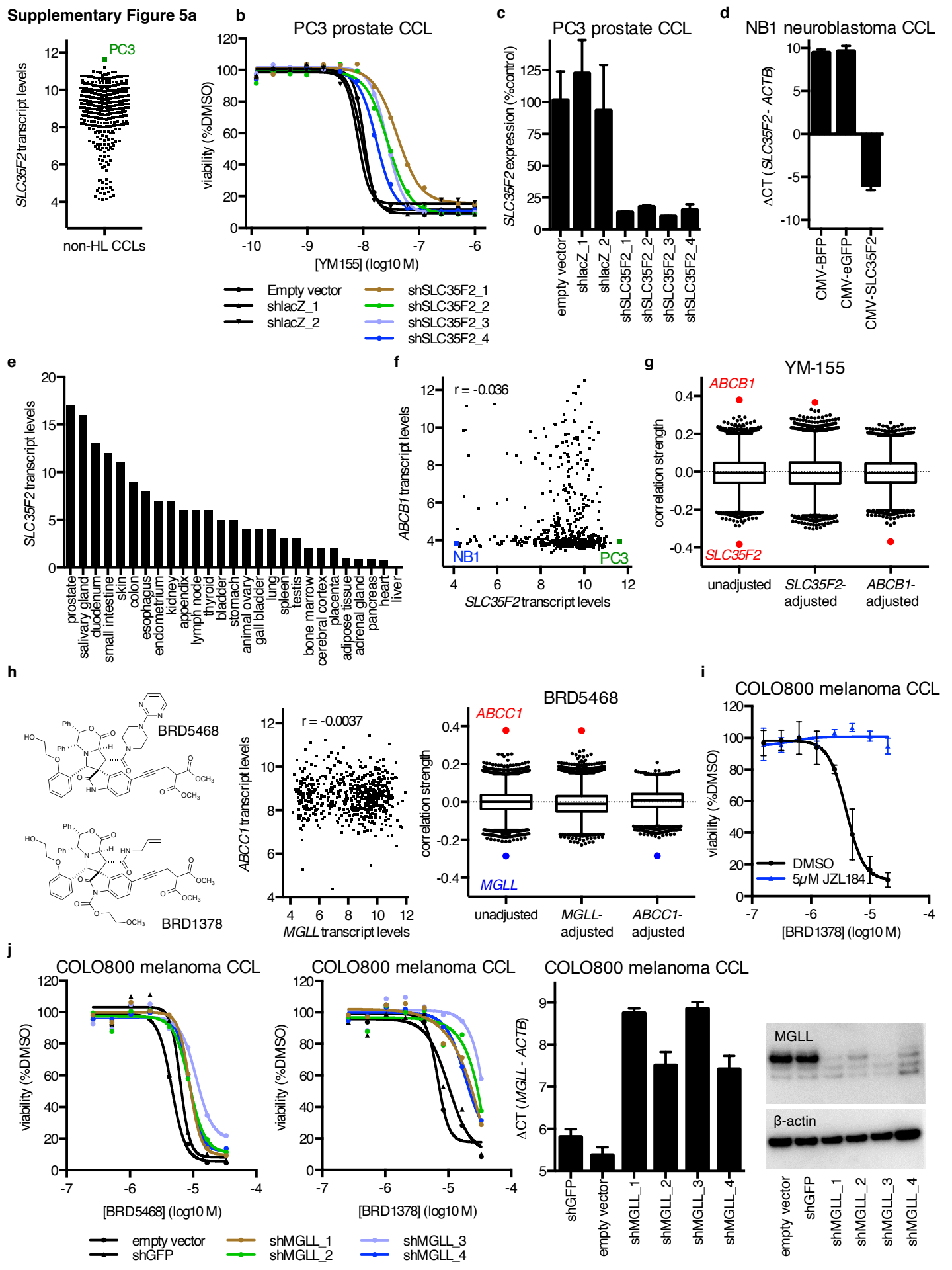

Supplementary Figure 5. MoA analysis reveals independent associations for YM-155 and BRD5468.

(**a**) Expression of *SLC35F2* across 601 non-HL CCLs assayed for YM-155 sensitivity. (**b**) Effects on YM-155 cytotoxicity upon knockdown of *SLC35F2* with four different hairpins in PC3 cells. Each point shows the mean of 2 independent experiments with 3 technical replicates each. (**c**) RT-PCR demonstrating *SLC35F2* transcript levels for knockdown in PC3 cells. Each bar represents mean + s.d. for n = 3. (**d**) RT-PCR demonstrating *SLC35F2* transcript levels for overexpression experiments in NB1 cells (**Fig. 3b**). Each bar represents mean + s.d. for n = 3. (**e**) RNA expression of *SLC35F2* across a normal human tissue panel (accession number E-MTAB-1733)[6]. See also supplementary reference [7]. (**f**) Co-expression plot for *ABCB1* and *SLC35F2* in non-HL CCLs. (**g**) Expression-sensitivity correlations for YM-155 with and without adjustment for *SLC35F2* or *ABCB1* expression using semi-partial correlation. Pearson correlations are shown. Boxplot outlier points represent Tukey outliers. (**h**) Chemical structures of BRD5468 and BRD1378, co-expression plot for *MGLL* and *ABCC1* in 615 non-HL CCLs assayed for BRD5468 sensitivity, and expression-sensitivity correlations for BRD5468 with and without adjustment for *MGLL* or *ABCC1* expression using semi-partial correlation. Pearson correlations are shown. Boxplot outlier points represent Tukey outliers. (**i**) Effects of co-treatment with DMSO or the MGLL inhibitor JZL184 on cytotoxicity of BRD1378 in COLO800 cells. Each point represents mean ± s.d. for n = 3 independent experiments. (**j**) Effects on BRD5468 and BRD1378 cytotoxicity upon knockdown of *MGLL* with four different hairpins in COLO800 cells, with each point the mean of 2 independent experiments, and RT-PCR and Western blot demonstrating *MGLL* transcript and protein levels for knockdown in COLO800 cells. Each bar represents mean + s.d. for n = 3. For uncropped gel image, see **Supplementary Figure 8c**.

Supplementary Figure 6a

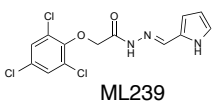

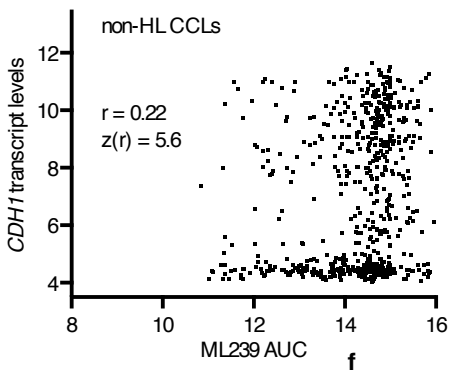

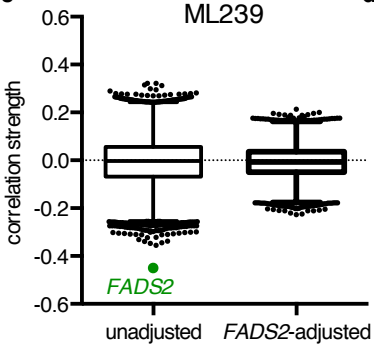

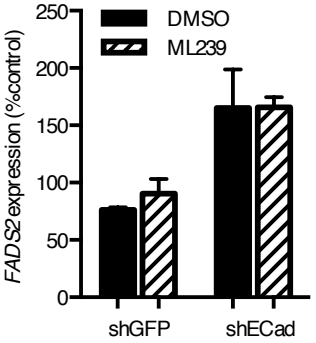

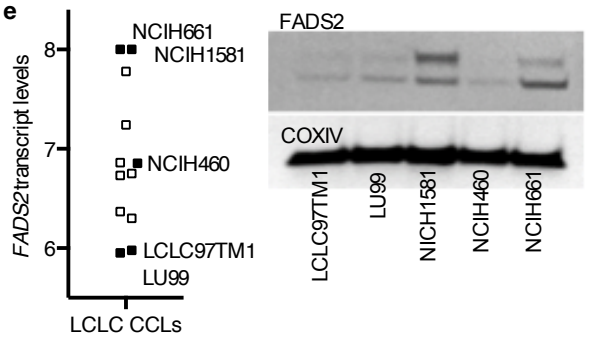

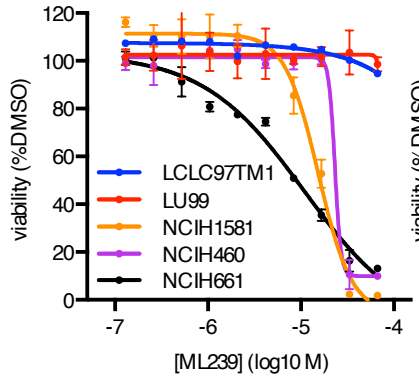

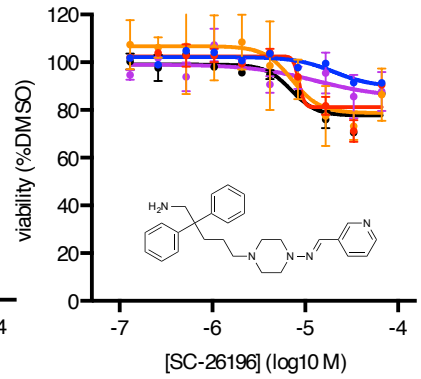

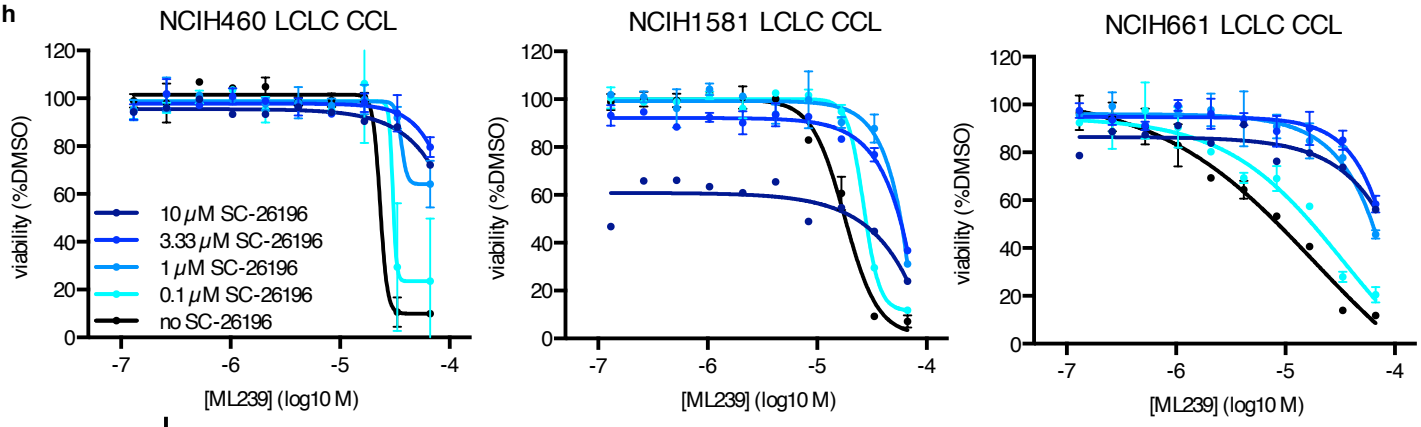

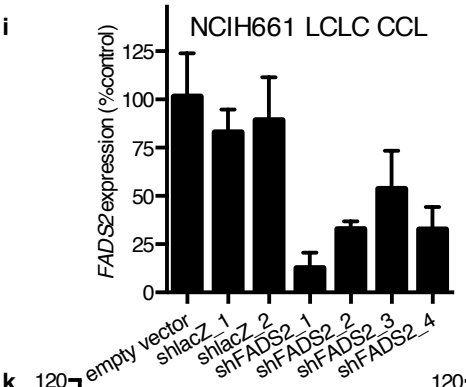

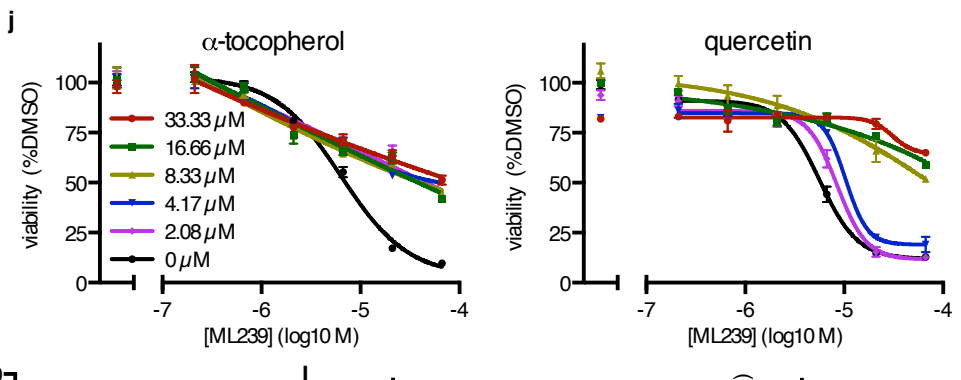

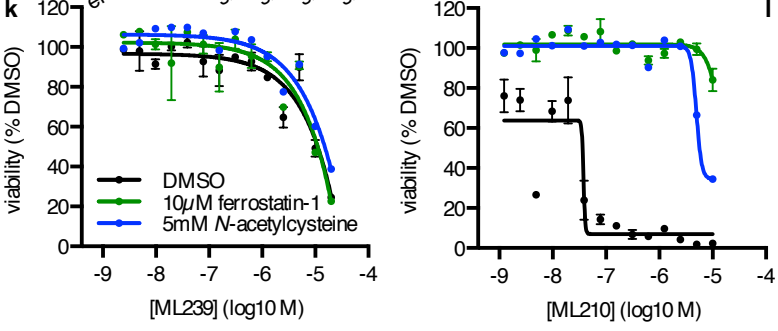

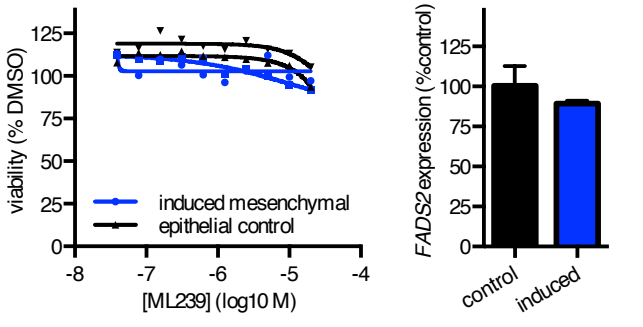

Supplementary Figure 6. FADS2 activity is required for ML239 cytotoxicity.

(**a**) Structure of ML239. (**b**) Scatterplot of ML239 AUC and *CDH1* levels in 645 non-HL CCLs. (**c**) Expression-sensitivity correlations for ML239 with and without adjustment for *FADS2* expression using semi-partial correlation. Pearson correlations are shown. Boxplot outlier points represent Tukey outliers. (**d**) mRNA expression of *FADS2* in shEcad-HMLE and shGFP-HMLE cells (data from GEO accession E-MTAB-884)[8]. Each bar represents mean + s.d. for n = 3. (**e**) Transcript levels of *FADS2* across large-cell lung carcinoma (LCLC) CCLs, with a subset of CCLs tested for FADS2 protein levels and (**f**) ML239 cytotoxicity indicated (filled black squares). For uncropped gel image, see **Supplementary Figure 8d**. (**g**) Structure and cytotoxicity profile of the FADS2 inhibitor SC-26196, and (**h**) effects of SC-26196 co-treatment on ML239 cytotoxicity in NCIH460, NCIH1581, and NCIH661 LCLC CCLs. Each point represents mean ± s.d. for n = 3 independent experiments. (**i**) RT-PCR demonstrating *FADS2* transcript levels for knockdown experiments in NCIH661 cells (see **Fig. 4c**). (**j**) Effects of α-tocopherol and quercetin co-treatment on ML239 cytotoxicity in NCIH661 cells. Each point represents mean ± s.d. for n = 3 independent experiments. (**k**) Effects of *N*-acetylcysteine or ferrostatin-1 co-treatment on ML239 or ML210 cytotoxicity in NCIH661 cells. Each point represents mean ± s.d. for n = 3 independent experiments. (**l**) Cytotoxicity of ML239 and RT-PCR demonstrating *FADS2* transcript levels in MCF7-ER-Snail-1^{6SA} cells either induced to undergo epithelial-to-mesenchymal transition (blue) or vehicle-treated (black). Each point shows the mean of 2 technical replicates. Two independent inductions are shown.

Supplementary Figure 7

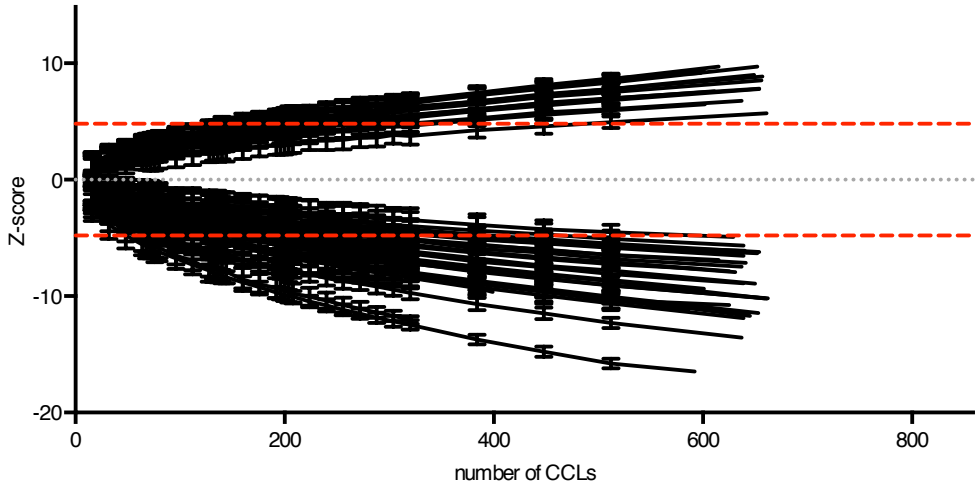

Supplementary Figure 7. Large numbers of CCLs are required to identify MoA.

Number of CCLs required to establish each of 43 connections in **Supplementary Table 1**. Red, Bonferroni-corrected Z-score cutoff ($|z| > 4.79$). See also **Figure 5**.

Supplementary Figure 8a

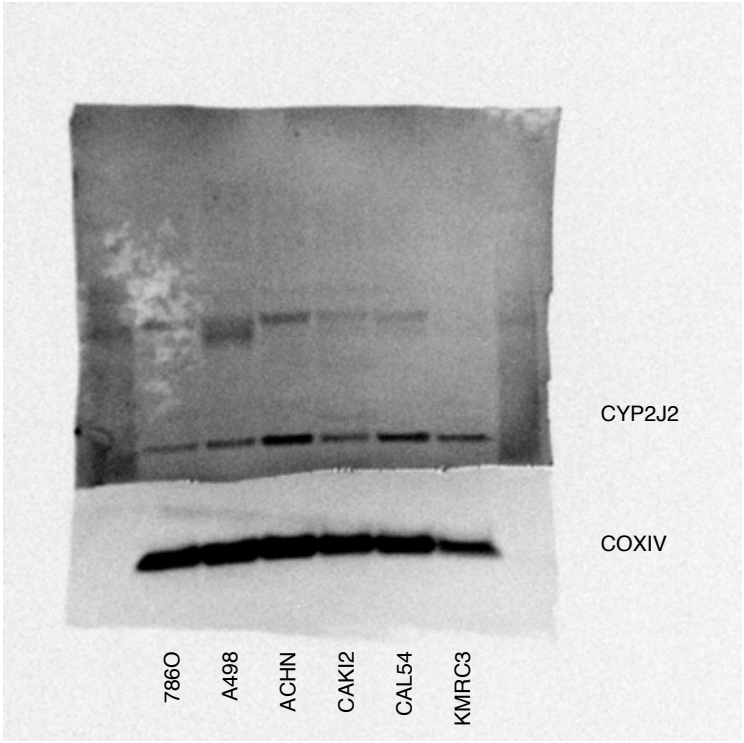

b

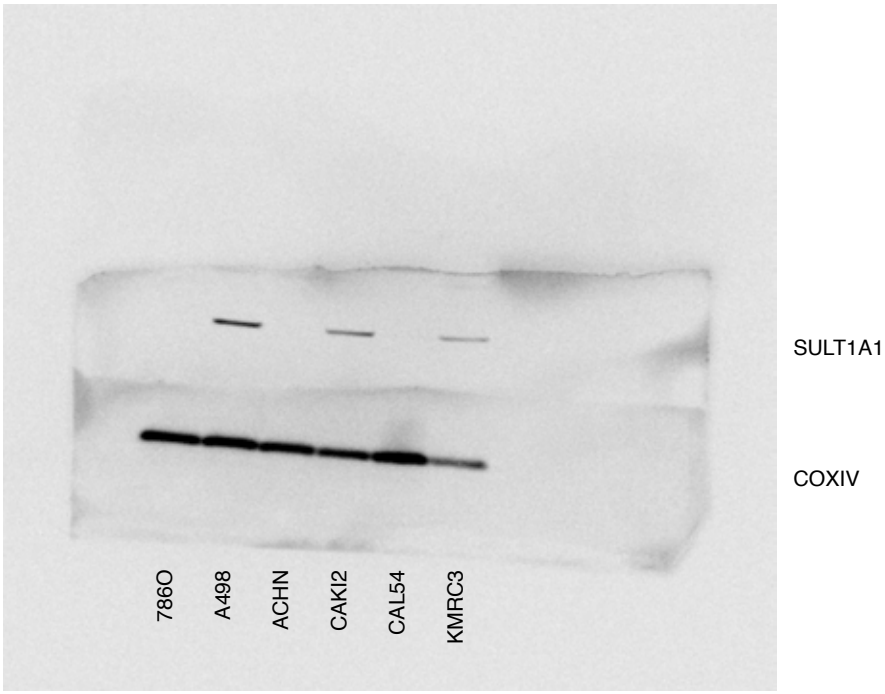

Supplementary Figure 8c

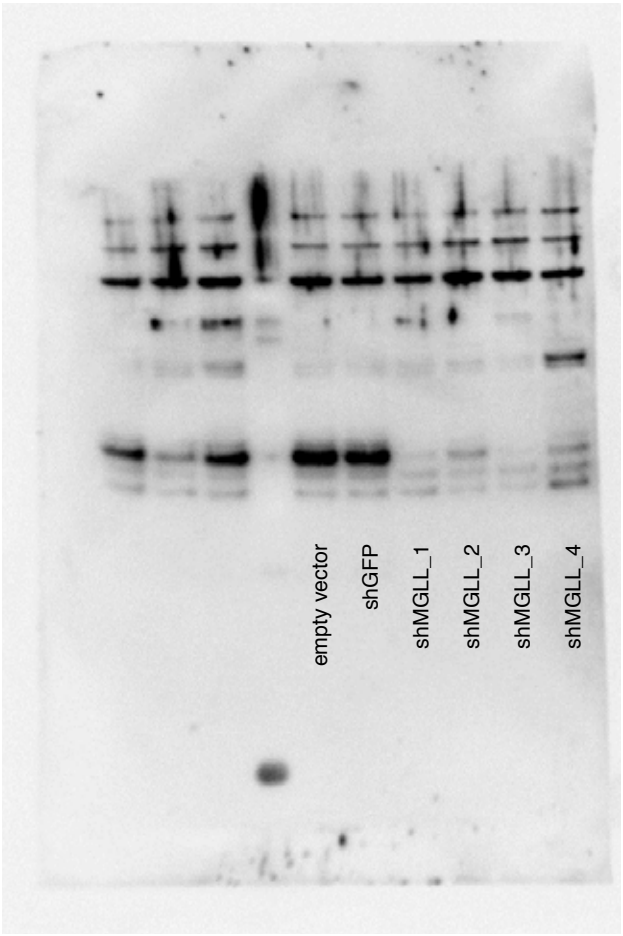

MGLL

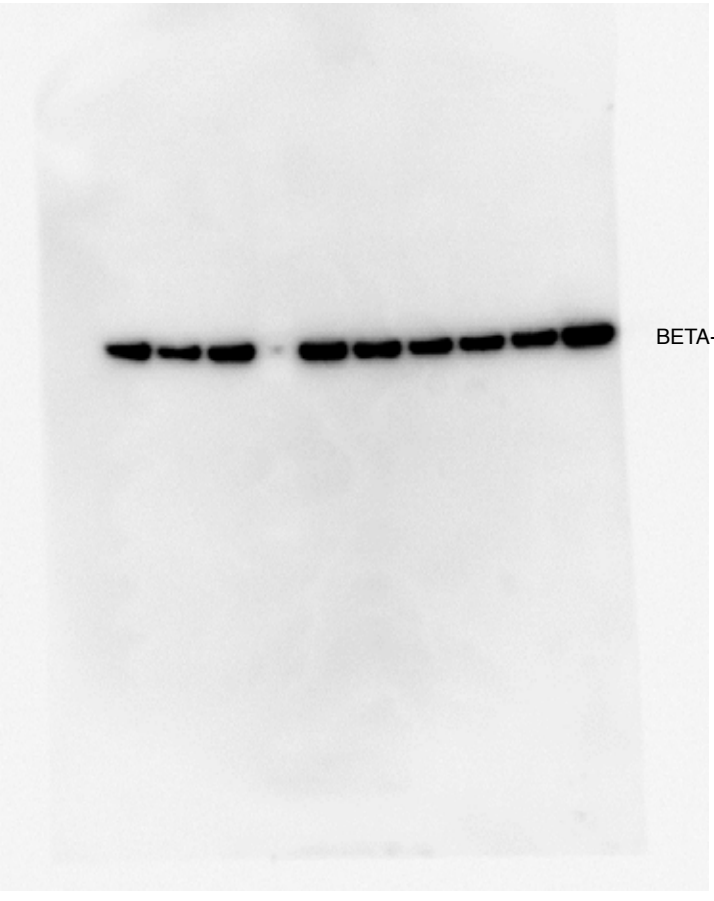

BETA-ACTIN

Supplementary Figure 8d

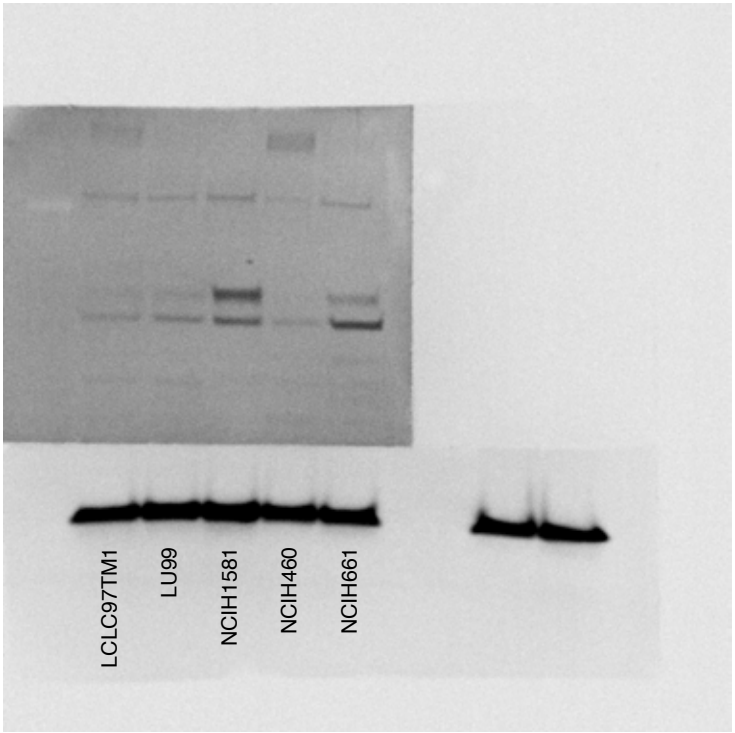

Supplementary Figure 8. Uncropped gel images for Western blots.

(**a**) Protein expression of CYP2J2 and COXIV in six renal CCLs. See also **Supplementary Figure 4a**. (**b**) Protein expression of SULT1A1 and COXIV in six renal CCLs. See also **Figure 2e**. (**c**) Protein expression of MGLL and beta-actin in COLO800 cells with shRNA knockdown of *MGLL* or control hairpins. See also **Supplementary Figure 5j**. (**d**) Protein expression of FADS2 and COXIV in five lung CCLs. See also **Supplementary Figure 6e**.

Supplementary References

1. Barretina, J. *et al*. The Cancer Cell Line Encyclopedia enables predictive modelling of anticancer drug sensitivity. *Nature* **483**, 603-7 (2012).
2. Guo, W. *et al*. Formation of 17-allylamino-demethoxygeldanamycin (17-AAG) hydroquinone by NAD(P)H:quinone oxidoreductase 1: role of 17-AAG hydroquinone in heat shock protein 90 inhibition. *Cancer Res* **65**, 10006-15 (2005).
3. Guo, W. *et al*. The bioreduction of a series of benzoquinone ansamycins by NAD(P)H:quinone oxidoreductase 1 to more potent heat shock protein 90 inhibitors, the hydroquinone ansamycins. *Mol Pharmacol* **70**, 1194-203 (2006).
4. Franceschini, A. *et al*. STRING v9.1: protein-protein interaction networks, with increased coverage and integration. *Nucleic Acids Res* **41**, D808-15 (2013).
5. Joseph, E.W. *et al*. The RAF inhibitor PLX4032 inhibits ERK signaling and tumor cell proliferation in a V600E BRAF-selective manner. *Proc Natl Acad Sci U S A* **107**, 14903-8 (2010).
6. Fagerberg, L. *et al*. Analysis of the human tissue-specific expression by genome-wide integration of transcriptomics and antibody-based proteomics. *Mol Cell Proteomics* **13**, 397-406 (2014).
7. Nishimura, M., Suzuki, S., Satoh, T. & Naito, S. Tissue-specific mRNA expression profiles of human solute carrier 35 transporters. *Drug Metab Pharmacokinet* **24**, 91-9 (2009).
8. Germain, A.R. *et al*. Identification of a selective small molecule inhibitor of breast cancer stem cells. *Bioorg Med Chem Lett* **22**, 3571-4 (2012).
9. Zoppoli, G. *et al*. Putative DNA/RNA helicase Schlafen-11 (SLFN11) sensitizes cancer cells to DNA-damaging agents. *Proc Natl Acad Sci U S A* **109**, 15030-5 (2012).
10. Johansson, P., Pavey, S. & Hayward, N. Confirmation of a BRAF mutation-associated gene expression signature in melanoma. *Pigment Cell Res* **20**, 216-21 (2007).